A Simulation of the January Standing Wave Pattern Including the Effects of Transient Eddies

J. D. OPSTEEGH[1] AND A. D. VERNEKAR

Department of Meteorology, University of Maryland, College Park 20742

(Manuscript received 17 June 1981, in final form 7 December 1981)

ABSTRACT

A steady-state, linear, two-level primitive equation model is used to simulate the January standing wave pattern as a response to mountain, diabatic and transient eddy effects. The model equations are linearized around an observed zonal mean state which is a function of latitude and pressure. The mountain effect is the vertical velocity field resulting from zonal mean wind over the surface topography. The diabatic heating is calculated using parameterized forms of the heating processes. The transient-eddy effects, i.e., the flux convergence of momentum and heat by transient eddies, are computed from observations. Separate responses of the model are computed for each of the three forcing functions.

The amplitude of the response to diabatic heating is small compared to observed values. The vertical structure is highly baroclinic. At the upper level, the phase of the waves is approximately in agreement with the observations. The amplitude of the response to mountain forcing is comparable with observations. The wavelength of the response in the Pacific sector is shorter than observed. The vertical structure is equivalent barotropic. The combined response to diabatic heating and mountain forcing is dominated by the contribution from the mountains. The phase shows some agreement with the observations, but the Aleutian low is located too far to the west and an unrealistic high appears to the west of the dateline.

The amplitude of the response to transient eddy effects is comparable to the observations in middle and low latitudes. At high latitudes the amplitudes are much too large. The assumption of linearity is not valid for strong forcing at high latitudes where the zonal wind is very weak. The vertical structure of the response is almost equivalent barotropic.

A comparison of the responses to mountain and transient eddy effects shows an interesting phase relationship. The troughs produced by the transient forcing are found in the lee of the troughs produced by the mountains (very close to the ridge) indicating that transient forcing is organized by the mountain effects.

The combined model response to all three forcing functions shows good agreement with observations except at very high latitudes.

1. Introduction

The quasi-stationary wave pattern on monthly or seasonal mean maps of the atmospheric circulation is often interpreted as an atmospheric response to forcing from the earth's surface. This forcing is mainly due to effects of surface terrain and diabatic heating resulting from the different thermal properties of continents and oceans. However, the equations for the stationary waves derived from the time-averaged equations for atmospheric flow, with a time-averaging period of a month to a season, show the influence of transients on the quasi-stationary waves as an additional force in the momentum equations and as additional heating in the thermodynamic equation (see, e.g., Saltzman, 1968). Various observational studies dealing with the time-averaged equations suggest that this forcing of quasi-stationary waves by transient eddies is an important process (Saltzman, 1962; Holopainen, 1973; Lau, 1979; Opsteegh and van den Dool, 1979).

Numerous studies have been made to simulate the quasi-stationary wave pattern as a response to mountain effects or diabatic heating effects or both (Charney and Eliassen, 1949; Smagorinsky, 1953; Döös, 1962; Saltzman, 1965; Sankar Rao and Saltzman, 1969; Derome and Wiin-Nielsen, 1971; and others). The earlier models used for these simulations had a very crude meridional structure. The earth's geometry was simplified to a β-plane and the zonal mean state, around which the equations were linearized, was independent of latitude. Consequently only the midlatitude standing wave pattern was simulated and the meridional structure of the waves was neglected. However certain assumptions about the meridional scale of the waves had to be made. Saltzman (1965) and Derome and Wiin-Nielsen (1971) found that their solutions were very sensitive to the particular choice of the meridional scale parameter, which means that this parameter can be used to tune the solutions with the observations. Recent investigations

[1] On leave from Royal Dutch Meteorological Institute.

0022-4928/82/040734-11$06.75

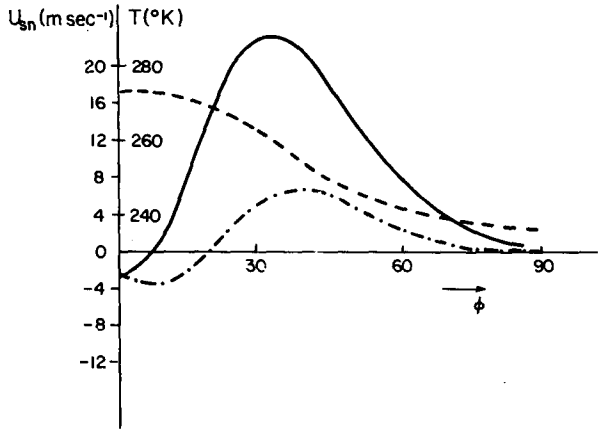

FIG. 1. The January mean zonally averaged wind at 400 mb (solid line) and 800 mb (dashed-dotted line) and the zonal mean temperature at 600 mb (dashed line) as a function of latitude.

used more complicated models, including a realistic zonal mean state and earth geometry (Egger, 1976b; Ashe, 1979). The results with these models show some agreement with the observed standing eddy pattern, especially in the upper part of the troposphere. But large errors in the phase of the waves occur as well. Recently, Youngblut and Sasamori (1980) simulated the influence of internal forcing with a linear steady-state model. They computed this eddy forcing from observations. Their model results indicate that the role of internal forcing in generating the quasi-stationary waves is important. However, their results are inconclusive because they do not try to simulate the standing eddy pattern with independent estimates of the various forcing mechanisms involved.

The purpose of this study is to simulate the quasi-stationary waves as a response to mountain and diabatic heating, and transient eddy effects. We use a linear steady-state two-layer primitive-equation model. The mountain effects are the vertical velocities produced by the zonal mean wind over the surface topography. Diabatic heating processes are calculated using parameterized forms of the heat fluxes. The transient eddy effects are computed from observations based on a five-year data set.

In the next two sections we briefly describe the model and computations of the forcing functions. Section 4 presents the results of the separate and combined responses of the model to all three forcing functions.

The response of the model to the mountain- and transient-eddy effects show an interesting relationship, suggesting a possibility of parameterizing the transient-eddy effects in terms of mountain effects. The combined response of the model to all the forcing functions is in good agreement with the observations except at very high latitudes.

2. The model

The model used in this study is described in detail in Opsteegh and van den Dool (1980). However, for the convenience of the reader only the important features are presented here. The model equations are derived from the time-averaged primitive equations on a sphere with an averaging time of one month. The tendency terms in these equations are neglected because they are small compared to the other terms in the equations (Opsteegh and van den Dool, 1979). The time-averaged variables are resolved into two components: zonal average and departures from zonal average (stationary waves). The equations are simplified by linearizing around the zonally-averaged basic state. This basic state depends on latitude and pressure, and is prescribed from observations. The data were kindly supplied by Dr. A. H. Oort. It is the zonal mean state for the years 1969–73. Fig. 1 shows the zonal mean state as a function of latitude. It is the zonal mean wind at 800 and 400 mb and the zonal mean temperature at 600 mb. The static stability at 600 mb is also a parameter of the mean state. It varies only slightly with latitude. Its hemispheric average value is $\sim 5.5\ 10^{-4}$ kPa^{-1}.

The linear system of equations for stationary waves as used in Opsteegh and van den Dool (1980) is as follows:

ZONAL MOMENTUM BALANCE

$$\frac{U_{sn}}{a\cos\phi}\frac{\partial \hat{u}}{\partial \lambda} + \frac{\partial U_{sn}}{a\partial\phi}\hat{v} + \frac{\partial U_{sn}}{\partial p}\hat{\omega} - f\hat{v} + \frac{1}{a\cos\phi}\frac{\partial \hat{\Phi}}{\partial \lambda} - \hat{F}_{Wx} = \hat{F}_{Ex} \quad (1)$$

MERIDIONAL MOMENTUM BALANCE

$$\frac{U_{sn}}{a\cos\phi}\frac{\partial \hat{v}}{\partial \lambda} + f\hat{u} + \frac{1}{a}\frac{\partial \hat{\Phi}}{\partial \phi} - \hat{F}_{Wy} = \hat{F}_{Ey} \quad (2)$$

FIRST LAW OF THERMODYNAMICS

$$\frac{U_{sn}}{a\cos\phi}\frac{\partial \hat{T}}{\partial \lambda} + \frac{\partial T_{sn}}{a\partial\phi}\hat{v} - \sigma_{sn}\hat{\omega} = \frac{\hat{Q}}{C_p} + \hat{Q}_E \quad (3)$$

CONTINUITY EQUATION

$$\frac{1}{a\cos\phi}\frac{\partial \hat{u}}{\partial \lambda} + \frac{1}{a\cos\phi}\frac{\partial}{\partial\phi}(\hat{v}\cos\phi) + \frac{\partial \hat{\omega}}{\partial p} = 0 \quad (4)$$

HYDROSTATIC APPROXIMATION

$$\frac{\partial \hat{\Phi}}{\partial \phi} = -\hat{\alpha} \quad (5)$$

EQUATION OF STATE

$$p\hat{\alpha} = R\hat{T} \quad (6)$$

Here U_{sn}, T_{sn} and σ_{sn} are the zonal mean wind, temperature and static stability respectively. The model

variables for the stationary planetary waves are $\hat{u}$, $\hat{v}$, $\hat{\omega}$, $\hat{\Phi}$, $\hat{T}$, $\hat{\alpha}$. These symbols have their conventional meaning. $\hat{F}_{Wx}$ and $\hat{F}_{Wy}$ are the dissipation terms. These terms are specified below. $\hat{F}_{Ex}$, $\hat{F}_{Ey}$ and $\hat{Q}_E$ are the internal sources of momentum and heat. $\hat{Q}$ is the diabatic heating.

The vertical discretization of the model is shown in the upper part of Fig. 2. The momentum equations and the continuity equation are applied at 400 and 800 mb, while the thermodynamic equation is applied at 600 mb. The upper and lower boundaries are at 200 and 1000 mb, where we assume that the vertical velocity vanishes, except when mountain forcing is considered. In that case, the vertical velocity produced by the surface airflow over the mountains is taken as the lower boundary condition.

The variables as well as the forcing components are expanded in Fourier series along a latitude circle. This leads to sets of equations in terms of Fourier coefficients, which can be solved for each of the zonal waves independently. We arrive at the total model response by adding the response for the individual zonal wavenumbers. Only the first five zonal wavenumbers are retained in this study. Higher wavenumbers give a negligible contribution to the total geopotential height response (Opsteegh and van den Dool, 1980).

In meridional direction a gridpoint representation is used with 23 gridpoints between the Equator and the North Pole. The grid is shown in the lower part of Fig. 2. A staggered grid system is used. $\hat{\omega}$ and $\hat{u}$ are defined at the gridpoints, whereas $\hat{\Phi}$ and $\hat{v}$ are formulated at intermediate points, indicated with open circles. The boundary conditions are

$$\left.\begin{aligned} \hat{v}\cos\phi &= 0 \quad \text{at} \quad \phi = \pi/2 \\ \frac{\partial\hat{\Phi}}{\partial\phi} &= 0 \quad \text{at} \quad \phi = 0 \end{aligned}\right\}, \tag{7}$$

where $\hat{v}\cos\phi$ is a variable which is used in the model instead of $\hat{v}$.

At the lower level of the model we have friction terms that are linear functions of the perturbation velocities. Following Egger (1976a), we also incorporate the vertical exchange of momentum. The resulting equations for $\hat{F}_{W_x}$ in the zonal momentum equations are

$$\hat{F}_{Wx3} = K_D(\hat{u}_1 - \hat{u}_3) - K_W\hat{u}_3\,, \tag{8}$$

$$\hat{F}_{Wx1} = -K_D(\hat{u}_1 - \hat{u}_3), \tag{9}$$

where the subscript 1 refers to 400 and 3 to 800 mb. K_D and K_W are vertical diffusion and surface friction coefficients respectively. They are constants in the model. The numerical value used for the friction coefficient is 2×10^{-6} s^{-1}. The value for the vertical diffusion coefficient is 1×10^{-7} s^{-1}. The friction terms in the meridional momentum equation (2) are obtained by replacing $\hat{u}_1$ and $\hat{u}_3$ by $\hat{v}_1$ and $\hat{v}_3$ in (8) and (9).

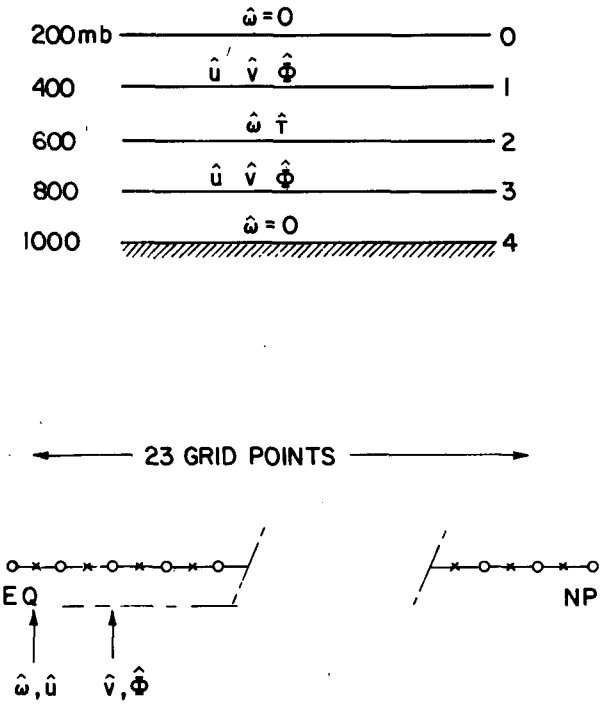

FIG. 2. Discretization of the two-level model in the vertical (upper part) and in the meridional direction (lower part).

3. The forcing functions

The diabatic heating resulting from inhomogeneities in the earth's surface is accounted for by using parameterizations for the various physical processes involved. These processes are shortwave radiation, longwave radiation, small-scale convection, evaporation and condensation, and subsurface conduction and convection. We adopted the parameterizations of these processes from Vernekar and Chang (1978). The validity of the parameterizations is discussed in various papers (Smagorinsky, 1963; Saltzman, 1967; Vernekar, 1975). The heating is dependent on surface temperature and albedo, atmospheric temperature and albedo, radiation–convection parameters and subsurface temperature. The heating scheme treats the surface and atmospheric temperatures as dependent variables of the model and other quantities are derived from observations. We take atmospheric temperature at 600 mb which is the dependent variable of the model. To determine the surface temperature we use the heat balance condition at the earth's surface. The heating in the atmospheric column $\hat{Q}_2$ can be expressed as

$$\hat{Q}_2 = A(\phi)\hat{T}_2 + B(\phi, \lambda). \tag{10}$$

The first part of the right-hand side of (10) is a

Newtonian cooling term and is dependent on the solution. The second part is fixed. For details on the derivation of (10) the reader is referred to Vernekar and Chang (1978). As the Newtonian cooling term also acts on the temperature perturbations created by mountain forcing and internal transient forcing, the resulting diabatic heat forcing is not the same when these processes are neglected. Nevertheless the diabatic heating is very much dominated by the fixed part of (10) so that this dependence of $\hat{Q}_2$ on the other forcing processes is not large. Fig. 3 shows the diabatic heating rate when the forcing due to mountains and transient eddies is neglected. The figure shows cooling over the continents and warming over the oceans, with maximum warming close to the east coasts of the continents. The distribution of the heating is in good agreement with estimates of this quantity by Lau (1979). The heating rate is of the order of 1 K day^{-1}, which is smaller than the values given by Lau. This is because Lau's estimates are for the total heating whereas Fig. 3 shows only the departures from the zonal average.

The effects of mountains on the standing eddies is introduced via a vertical velocity at the lower boundary. We use

$$\hat{\omega}_4 = \frac{-\bar{\rho}_4 U_{sn}}{a\cos\phi}\frac{\partial gH}{\partial\lambda} \tag{11}$$

to determine the vertical velocity at the lower boundary. U_{sn} is the zonal mean wind at a representative level, which is taken to be the 900 mb level. H is the topographic height which is shown in Fig. 4.

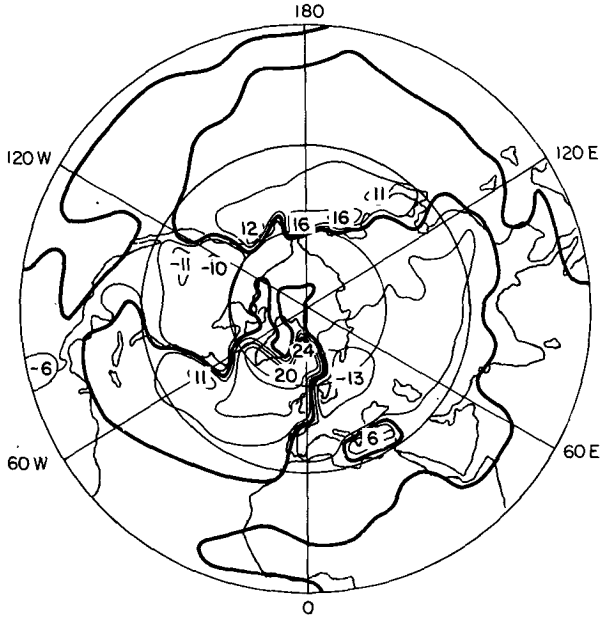

FIG. 3. Computed asymmetric component of the January mean heating at 600 mb in 10^{-1} K day^{-1}. Contour interval is 0.5 K day^{-1}.

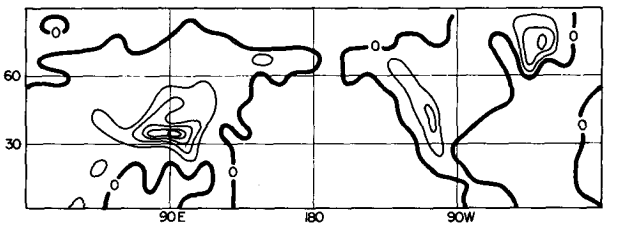

FIG. 4. Large-scale features of the topography of the Northern Hemisphere. Contour interval is 1000 m.

The transient forcing is computed from observational data. The data came from the same data set that was used for the computation of the zonal symmetric state. So it is the mean January internal forcing for the years 1969–73. The forcing can be written in terms of the convergence of eddy fluxes of momentum and heat as follows:

$$\hat{F}_{Ex} = -\left(\frac{1}{a\cos\phi}\frac{\partial\overline{u'^2}}{\partial\lambda} + \frac{1}{a}\frac{\partial\overline{u'v'}}{\partial\phi} + \frac{\partial\overline{u'\omega'}}{\partial p} - \frac{2\tan\phi}{a}\overline{u'v'}\right), \tag{12}$$

$$\hat{F}_{Ey} = -\left[\frac{1}{a\cos\phi}\frac{\partial\overline{u'v'}}{\partial\lambda} + \frac{1}{a}\frac{\partial\overline{v'^2}}{\partial\phi} + \frac{\partial\overline{v'\omega'}}{\partial p} + \frac{\tan\phi}{a}(\overline{u'^2} - \overline{v'^2})\right], \tag{13}$$

$$\hat{Q}_E = -\left(\frac{1}{a\cos\phi}\frac{\partial\overline{u'T'}}{\partial\lambda} + \frac{1}{a}\frac{\partial\overline{v'T'}}{\partial\phi} + \frac{\partial\overline{\omega'T'}}{\partial p} - \frac{R}{pC_p}\overline{\omega'T'}\right). \tag{14}$$

The data set contained five-year averages of $\overline{u'^2}$, $\overline{u'v'}$, $\overline{v'^2}$, $\overline{u'T'}$ and $\overline{v'T'}$. The data on vertical fluxes were not available. We therefore omitted the vertical fluxes in computing $\hat{F}_{Ex}$, $\hat{F}_{Ey}$ and $\hat{Q}_E$. Before computing the gradients in (12) to (14) the data were smoothed twice in ϕ direction with a three-point smoother. Because of the very large uncertainty in the eddy fluxes at high latitudes we interpolated $\hat{F}_{Ex}$, $\hat{F}_{Ey}$ and $\hat{Q}_E$ between 70°N and the pole such that the internal forcing components decrease linearly from 70°N to zero at the pole. Fig. 5 shows the distribution of the internal forcing components in the five model equations. In spite of the generally noisy character of these transient forcing fields they show some large preferred regions of convergence and divergence of momentum and heat. Because the model response to high zonal wavenumbers is always very small compared to that for low zonal wavenumbers, the response to these noisy forcing fields will be very much dominated by the large-scale pattern in these fields.

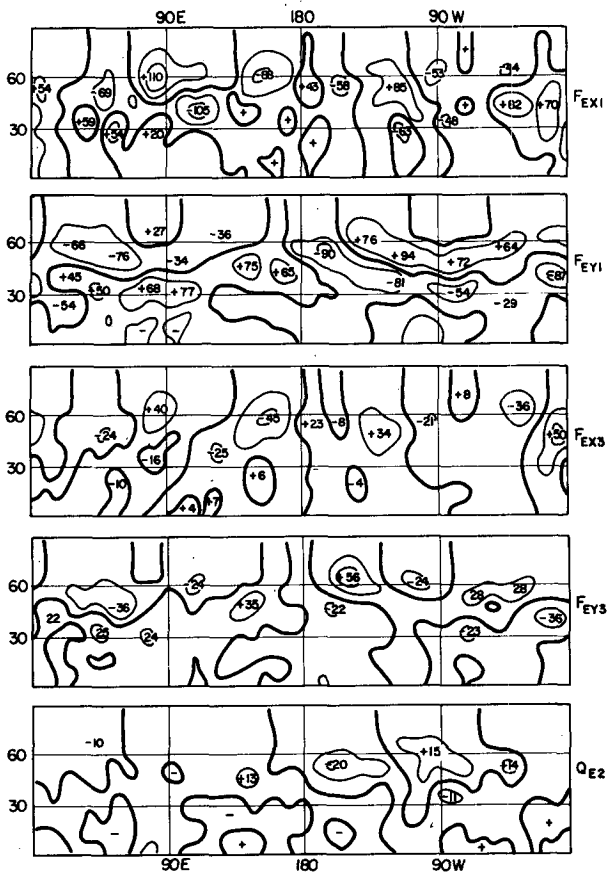

FIG. 5. Hemispheric distribution of the internal forcing by transient eddies. The upper two figures show the forcing in the zonal and meridional momentum equations at 400 mb respectively. The next two figures show the same forcing fields at 800 mb. The lower figure shows the forcing in the thermodynamic equation at 600 mb. Units are 10^{-6} m s^{-2} for the upper four figures and 10^{-6} K s^{-1} for the bottom figure.

4. Results

Fig. 6 shows the mean observed January standing eddy pattern at 400 and 800 mb. The data are from Crutcher and Meserve (1970). In zonal direction the pattern is very much dominated by wavenumbers up to three. In meridional direction it shows a nodal structure, with nodes in the subtropics, middle latitudes and high latitudes. The midlatitude node has the largest amplitude. The phase changes near 30°N are very large, so that the lows and highs at middle latitudes are always accompanied by pressure systems of opposite sign in the subtropics. We shall see to what extent the model is able to reproduce these observed characteristics of the standing eddy pattern.

In order to determine the relative importance of the various forcing components involved in the generation of the standing eddies we shall discuss the separate contribution of the forcing components.

a. Diabatic heating and mountain forcing

Fig. 7 shows the geopotential height response at 400 mb to the diabatic heating field. Apart from a rather large response at high latitudes which is probably an artifact of the linear model, the amplitudes of the pressure systems at middle latitudes is of the order of 5 to 10 geopotential dam. So the contribution of the heating to the observed midlatitude node of the standing eddy pattern is not very large. However, the phase of the waves is in good agreement with the observed highs along the west coasts and to the observed lows along the east coasts of the American and Eurasian continents.

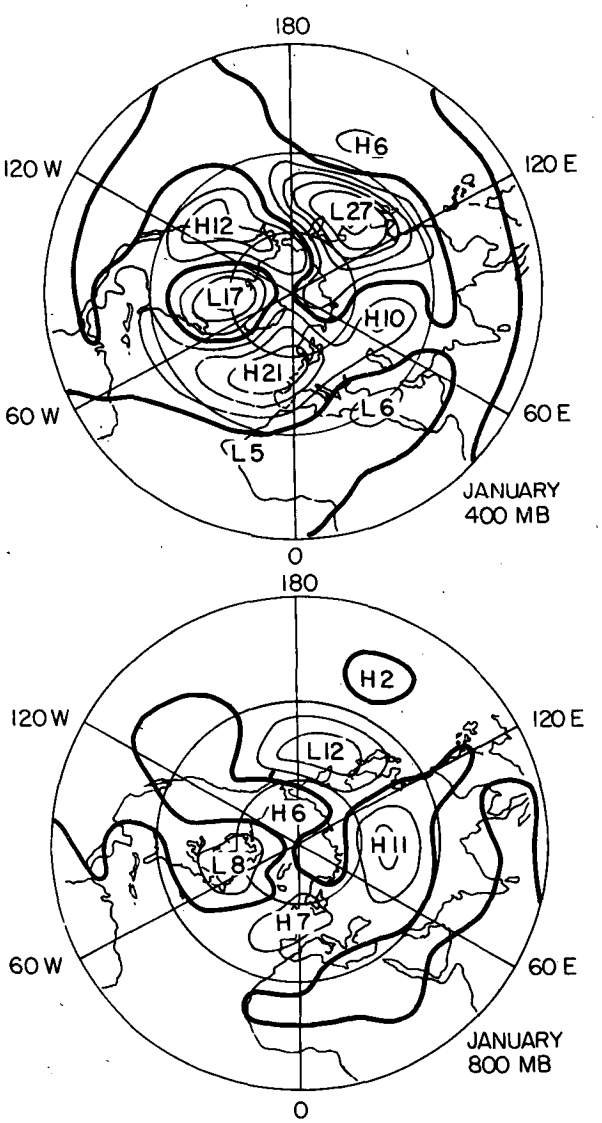

FIG. 6. Observed January standing eddy pattern at 400 and 800 mb. Units are in geopotential dam. The same units will be used in all the remaining figures. The zero line is indicated with a thick line. Contour interval is 5 geopotential dam.

Vernekar and Chang (1978) used the same heating parameterizations to simulate January quasi-stationary waves. The response of their model had approximately the same phase as in these results but the magnitudes were larger by a factor of two. Their model was based on quasi-geostrophic approximations and the zonally-averaged state was uniform with latitude. We made several experiments on both the models to determine the reason of the differences between these responses. It appears that the different quasi-resonant properties of the two models were responsible for the different results. The quasi-resonant modes for the quasi-geostrophic and PE models are wavenumbers 3 and 4, respectively. However, the resonant mode in the quasi-geostrophic model had the highest amplitude, whereas in the PE model its amplitude was relatively small compared to that of wavenumbers 1 and 2. In order to determine the sensitivity of the results in both models to the dissipative processes, we made the same experiment by increasing the friction coefficient by an order of magnitude. In the quasi-geostrophic model the amplitude of wavenumber 3 was reduced by a factor of two. As a result the cumulative response of all the waves was also reduced by a factor of two. In the PE model the amplitude of wavenumber 4 was also reduced, but the cumulative response of all the waves was not significantly affected.

The geopotential height perturbations in the tropics are very small. In Opsteegh and van den Dool (1980) it was shown that the balancing processes in the stationary waves are different for middle latitudes and tropics. In middle latitudes the perturbations are almost geostrophic and the balancing process is the horizontal advection. In the tropical easterlies the flow has the character of a direct thermal circulation, which is highly ageostrophic (Walker-type circulations). Here the balancing process is cooling (warming) in upward (downward) motions.

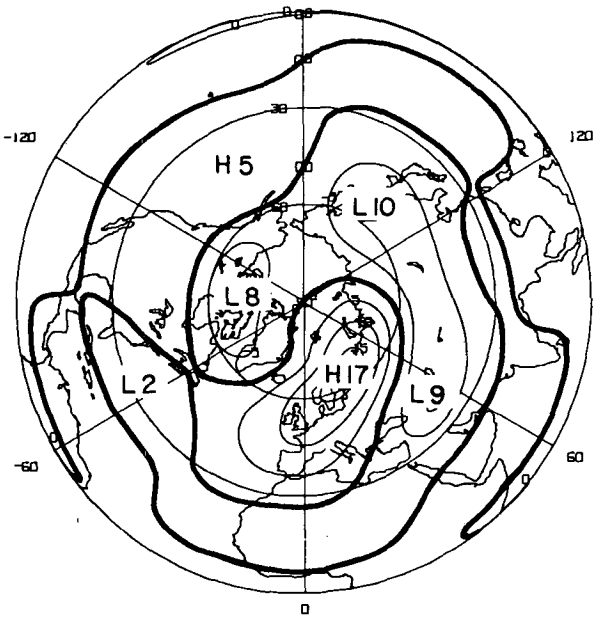

FIG. 7. Geopotential height response at 400 mb to diabatic heating.

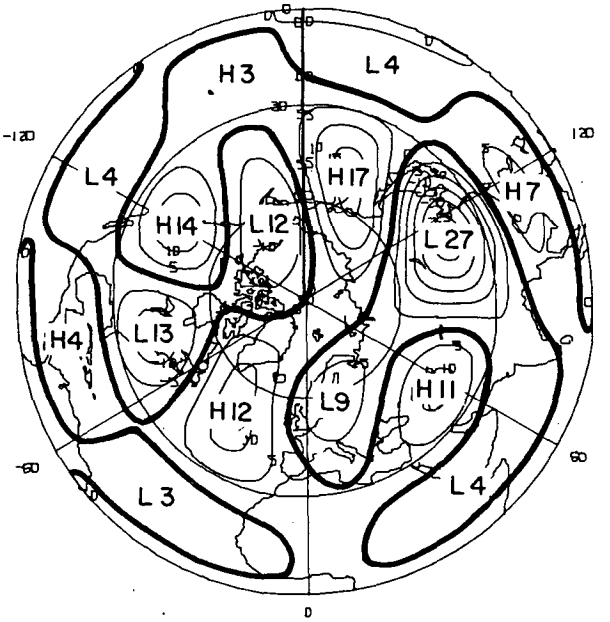

FIG. 8. Geopotential height response at 400 mb to topographic forcing.

Fig. 8 shows the 400 mb height field simulated using orographic forcing. The amplitudes of these results are much closer to the observations as compared to those forced by the heat sources and sinks. This is in agreement with the results of several other studies, which suggest that the effect of orographic forcing is dominant at middle and higher tropospheric levels (Charney and Eliassen, 1949; Derome and Wiin-Nielsen, 1971; Manabe and Terpstra, 1974). The diabatic heating may be important for the observed surface lows and highs. It was shown by Smagorinsky (1953) and recently by Hoskins and Karoly (1981) that the pressure distribution near the surface is extremely sensitive to diabatic heat sources and sinks at low altitudes, whereas the response at upper levels is probably more determined by the vertically-averaged heating. These shallow heating effects cannot be dealt with in the present two-level model and therefore we cannot expect to simulate more than the mid- and upper-tropospheric standing wave pattern.

Comparison between Fig. 8 and the observed standing eddy pattern (Fig. 6) shows that the sim-

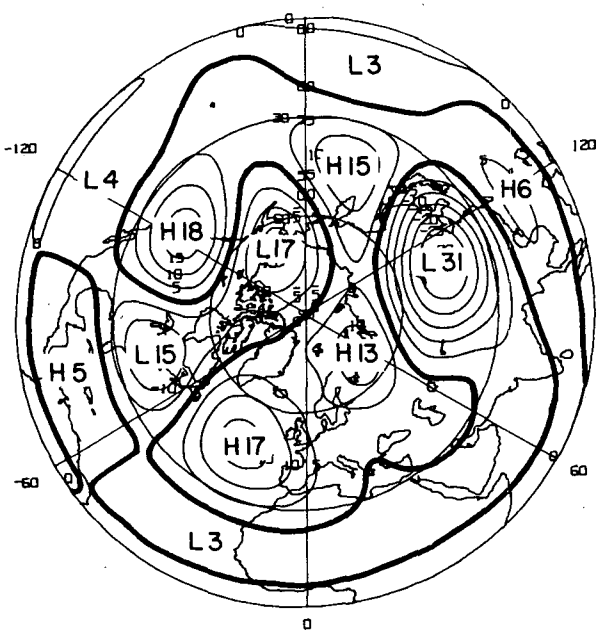

FIG. 9. Geopotential height response at 400 mb to both diabatic heating and topographic forcing.

ulated mountain effect has a shorter wavelength than observed, especially in the Pacific sector. This was also found by Hoskins and Karoly (1981). In fact these results show a very close agreement with their results for mountain forcing, which were obtained with a five-level steady-state primitive-equation model, suggesting that the results are not very sensitive to the vertical resolution of the model. Fig. 8 shows a fair agreement with the observations for the low and high associated with the Rockies. However the low over Western Europe and the high west of the date line are not observed. The Aleutian low is located too far to the west.

Fig. 9 shows the combined effects of heat and orographic forcing at 400 mb. Because of the relative importance of orographic forcing, the results are not much different from Fig. 8. However, the unrealistic low over Western Europe, produced by the effects of mountains is counteracted by the heating and has disappeared in the combined results.

b. Internal forcing by transient eddies

The effect of internal forcing by transient eddies is shown in Fig. 10. In middle latitudes and subtropics the pressure systems have amplitudes that are comparable with the observed values. However, the amplitude of the high-latitude node of the wave pattern is unrealistically large. Here we see a serious drawback of the assumption of linear behavior of stationary planetary waves. In spite of the fact that we modified the transient forcing by decreasing it linearly to zero from 70°N to the North Pole, the forcing still has considerable strength at high latitudes. This forcing is balanced mainly by zonal advection. However, due to very small values of the zonal mean wind at high latitudes the resulting asymmetrical perturbation has to be large in order to balance the forcing fields. The tendency of creating large amplitudes at high latitudes could also be seen in the computation of the effect of diabatic heating. In his simulation of the January standing waves, Ashe (1979) computed the effects of heating and mountain forcing with a linear and a nonlinear model. One of the differences between the results of both models was that the linear model created large amplitudes at high latitudes but the nonlinear model did not.

Because of the unrealistic response of the linear model to forcing at high latitudes we cannot expect to be able to simulate the high-latitude node of the standing eddies with any degree of accuracy. It is interesting, however, to investigate to what extent the response at middle and low levels is determined by the high-latitude behavior of the wave pattern. We investigated this for small changes in the zonal mean wind at high latitudes. The amplitude of the response at high latitudes appeared to be very sensitive for these small changes. It could change by a factor of almost two. However the amplitude of the mid- and low-latitude nodes of the wave pattern changed only slightly. Here the changes amounted to a maximum of 20%. More importantly the phases of the waves were not at all affected. Although unrealistic behavior of the linear model due to strong

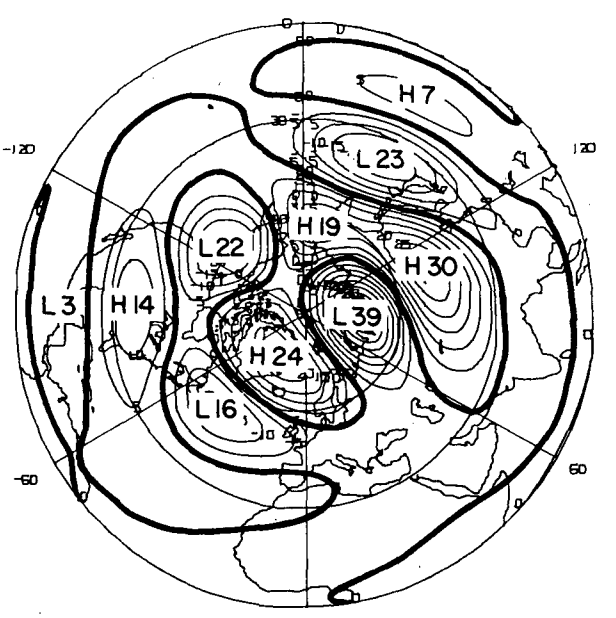

FIG. 10. Geopotential height response at 400 mb to internal forcing by transient eddies.

forcing at high latitudes creates some uncertainty in amplitude, we still have confidence in its ability to simulate the mid- and low-latitude effects of internal forcing.

c. *Analysis of midlatitude response*

Fig. 11 shows the geopotential height response at both levels along 45°N for the three forcing components separately and combined. The vertical structure of the midlatitude response to diabatic heating is highly baroclinic, whereas the response to orographic forcing has an equivalent barotropic structure. This is also true for the vertical structure of the perturbations due to internal forcing by transient eddies. Since the transient forcing consists partly of heating in the thermodynamic equation this result is a little bit surprising. Therefore we did two additional experiments with transient forcing. In one experiment we retain the forcing only in the momentum equations and in the second we retain only heat forcing. The results are shown in Fig. 12. The

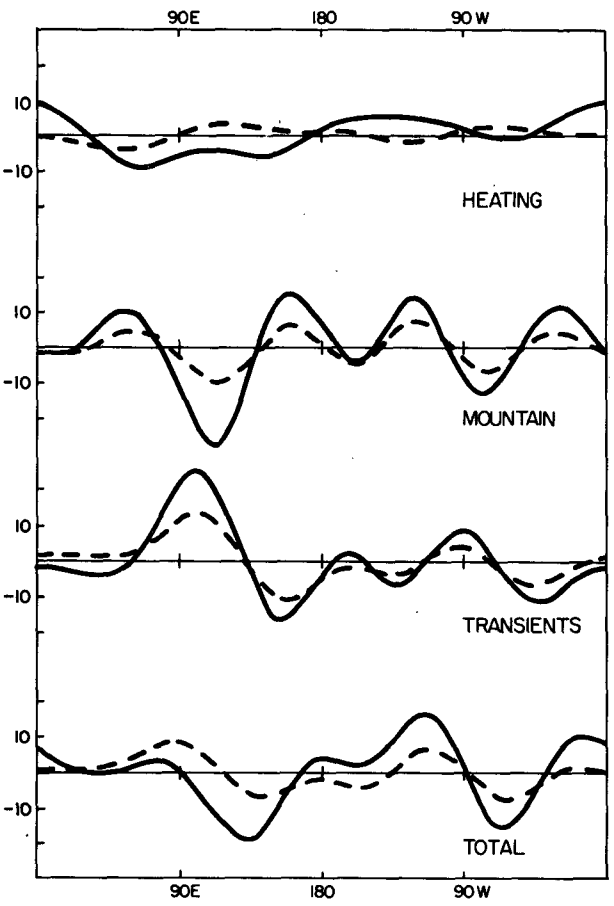

FIG. 11. Geopotential height response at 400 (solid line) and 800 mb (dashed line) along 45°N to the three forcing components separately and combined.

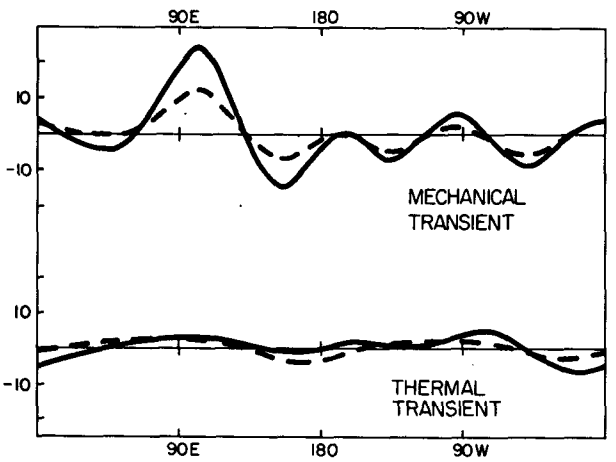

FIG. 12. Geopotential height response at 400 (solid line) and 800 mb (dashed line) along 45°N to the separate effects of transient forcing in the momentum equations and transient forcing in the thermodynamic equation.

eddy-flux convergence of momentum is much more important for the standing eddies than the convergence of eddy-heat flux, which explains the equivalent barotropic vertical structure of the total response. The small tilt that can be seen in the combined results is of course due to the effects of diabatic heating.

An interesting feature shows up in Fig. 11. Comparing the results for mountain and transient forcing it can easily be seen that there seems to exist a phase relationship between both wave patterns. The troughs produced by transient forcing are found without exception in the lee of the mountain-produced troughs, very close to the ridge. As it is well known that cyclogenesis generally occurs in the lee of the troughs of planetary waves, we may simply interpret these results as the statistical effect of deepening cyclones on the monthly mean pattern. Apparently, the internal forcing is organized by the externally-forced planetary waves. Lau and Wallace (1979) showed that the convergence of eddy flux of vorticity is connected to the mean winter surface lows and highs in such a way that the eddies simply act to maintain the surface-pressure systems against friction. Surface-heating processes may have a large impact on the location and depth of the surface lows and highs; however, it seems likely that the location of the surface-pressure systems is also partly determined by cyclogenetic processes aloft. The total picture of how the statistical effects of transient eddies are related to external heat and mountain forcing is not yet clear. Nevertheless, we believe that there is some indication that such a relation exists and that this might provide a way of parameterizing the effect of transient eddies on the mean flow in terms of the conditions at the earth's surface.

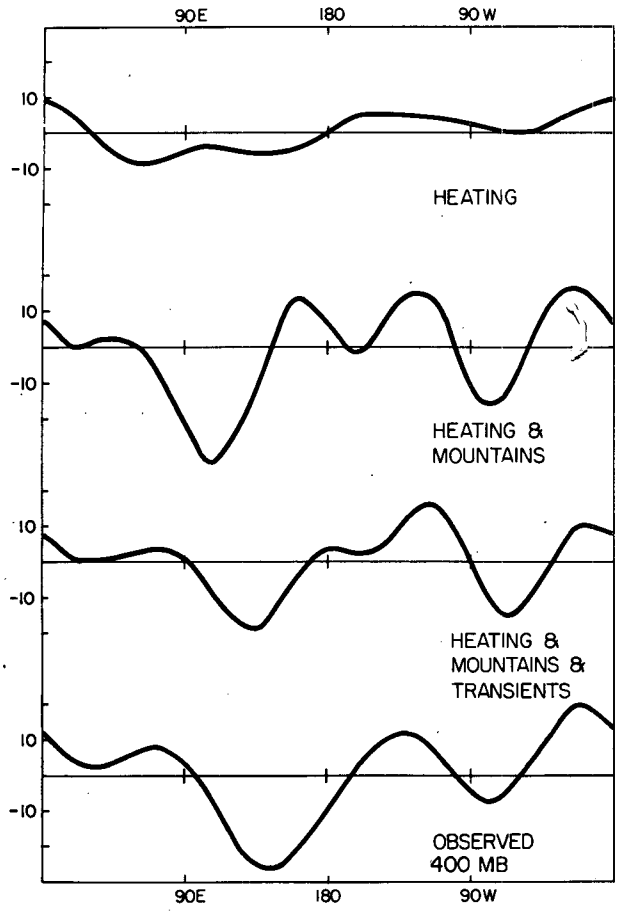

FIG. 13. Geopotential height response at 400 mb along 45°N. The upper curve gives the results for diabatic heating. The second curve gives the response to diabatic heating and mountain forcing. The third curve gives the response when all three forcing components are included. The lower curve gives the corresponding observed geopotential height at 400 mb.

d. Comparison with observations

First, we shall compare the results with the observed standing eddy pattern at middle latitudes. Fig. 13 shows the geopotential height at 45°N as a function of longitude. The upper part of the figure is the response to diabatic heat forcing. In the next curve the effect of mountains is added and finally the effect of the three forcing components is shown. The lower curve shows the observed wave pattern along 45°N. Again it can be seen that the heating contributes to the observed lows along the east coasts and to the observed highs along the west coasts of the American and Eurasian continents. Adding the effects of orographic forcing gives an amplitude that is comparable with the observed wave pattern. The main deficiencies are the unrealistic high to the west of the date line and the Aleutian low which is located too far to the west. Adding the effects of transient forcing eliminates the unrealistic high and causes the Aleutian low to shift to the east. The simulation is in very good agreement with the observed pattern shown by the bottom curve.

In Fig. 14 the results are presented for the lower level of the model (800 mb). The same arguments apply for the simulation at this level. Adding the effects of internal forcing eliminates the unrealistic high west of the date line and shifts the Aleutian low to the west. It is clear that, also on the 800 mb level, the transient forcing contributes much to the observed wave pattern. It seems to be especially important for the simulation of the Siberian high and the Aleutian low.

Figs. 15 and 16 show the simulated hemispheric wave pattern at 400 and 800 mb respectively for the experiment in which all three forcing components are included. The response is dominated by the high-latitude node which shows a strong wavenumber-2 pattern. As a consequence of the dominance of the high-latitude node the center of the midlatitude pressure systems have been pushed 5–8° south of the observed location. The correspondence between the middle latitudes and the subtropics is in good agreement with the observations (Fig. 6). The results show large

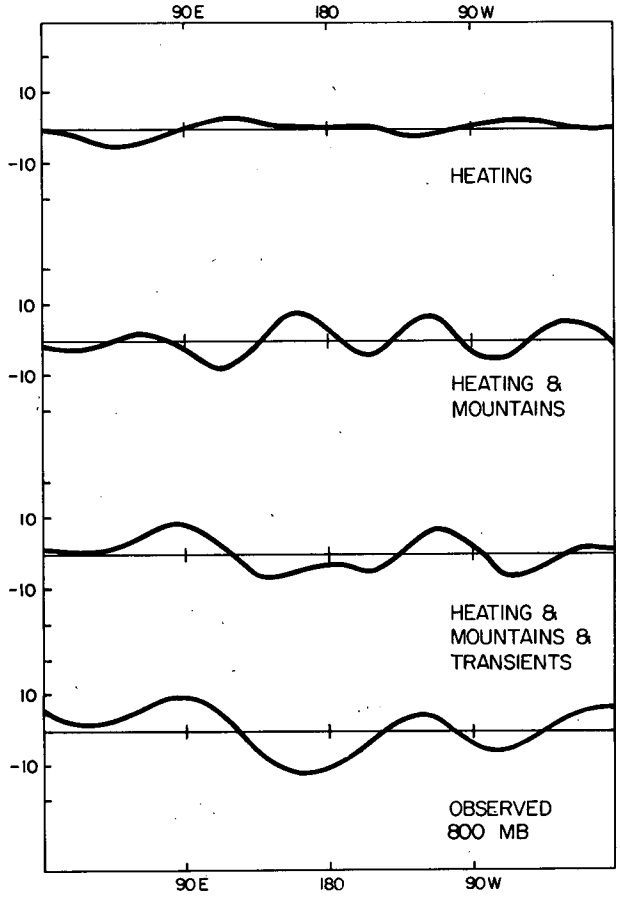

FIG. 14. As in Fig. 13 except for 800 mb.

phase changes at ~25°N so that the midlatitude lows and highs are always accompanied by a subtropical pressure system of opposite sign. The amplitude of the subtropical lows and highs is close to the observed values. As a quantitative measure of the agreement between observed and simulated results we computed correlation coefficients for both the levels. That is, we computed correlation coefficients between Fig. 6 (upper) and Fig. 15, and between Fig. 6 (lower) and Fig. 16 as a function of latitude. The hemispheric correlation coefficient was computed from these results as an area-weighted average. The squares of the correlation coefficients are 0.3 and 0.12 for the 400 and 800 mb levels, respectively. Even though the qualitative agreement appears fairly good there is much room for improvement in the model for a good quantitative agreement with observations.

5. Conclusions and discussion

We have shown that transient eddies have a large impact on the January standing wave pattern. In spite of the fact that forcing by inhomogeneities in the surface of the earth is strong enough to explain the observed amplitude of the standing eddies, the effect of internal forcing was needed to simulate the proper phase of the waves. This is especially true for the Siberian high and the Aleutian low.

Our results suggest that the statistical effect of transient eddies on the monthly mean flow is organized by the externally forced waves. There is a phase relation between the mountain-induced stationary wave and the internally forced wave. The troughs produced by the transients occurred downstream of the mountain troughs, close to the ridge. It is well known that the phase of planetary waves determines the areas that are favorable for cyclogenetic processes. It is believed that the simulation of the effect of transient eddies is a reflection of this organization of cyclogenetic activity. Lau and Wallace (1979) show from observations that the transient eddies act to maintain the winter mean surface lows and highs against the effect of friction. Therefore, the location of these pressure systems is possibly partly determined by cyclogenetic activity aloft.

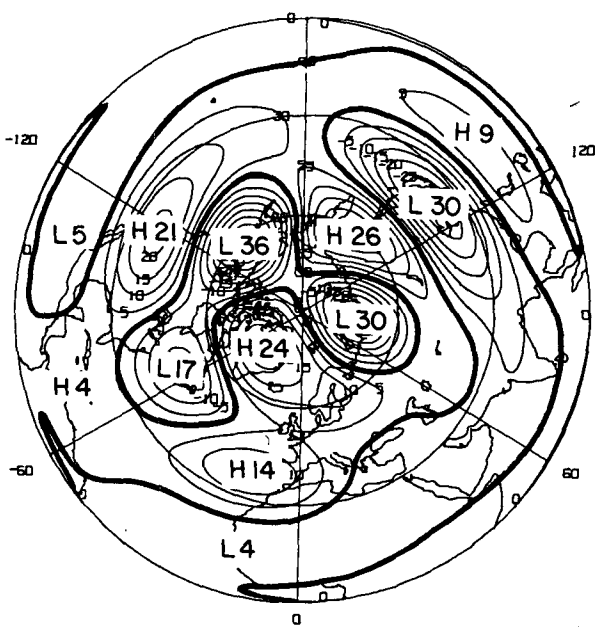

FIG. 15. Geopotential height response at 400 mb to diabatic heating, topographic forcing and internal forcing by transient eddies.

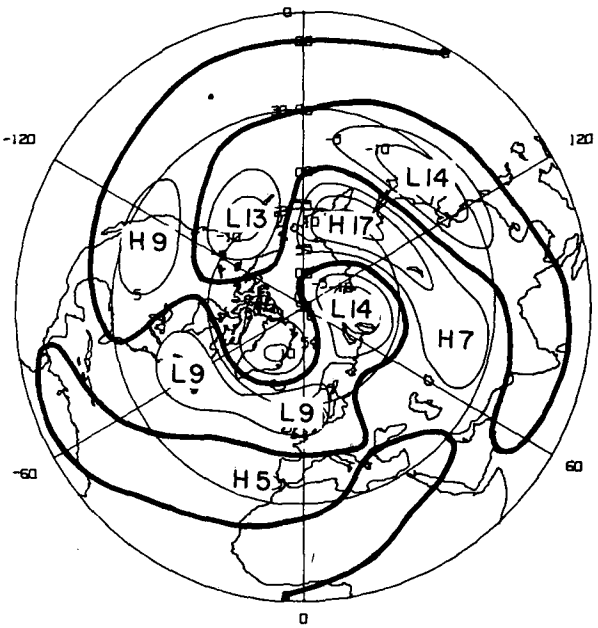

FIG. 16. As in Fig. 15 except for 800 mb.

The upper tropospheric effect of asymmetric diabatic heating from ocean–continent contrasts is probably somewhat smaller than the effects of mountains and transient eddies. However, it seems likely from the results of simulations with models that have a larger resolution in the vertical that heating may be very important for the mean surface-pressure systems.

The simulated wave pattern at middle and low latitudes shows a good agreement with observations, indicating that the assumption of linear behavior of stationary planetary waves is realistic. This was also shown by Lau (1979) from observations. The linearity assumption breaks down for strong forcing at high latitudes where the zonal mean wind is very small. In order to obtain a good simulation of the standing eddies at all latitudes nonlinear effects should be included. The results can be further improved by including more realistic mountain effects. While this study improves upon many previous stud-

ies by allowing for the variation of the zonal mean wind with latitude, it neglects the potentially important effects of meridional airflow over mountains that might be generated mainly by the surface heating component of the forcing (e.g., Saltzman and Irsch, 1972). In spite of the unrealistic behavior of the model at high latitudes, this study clearly demonstrates the role of internal forcing by transient eddies as compared to the external forcing by mountain and diabatic heating effects.

Acknowledgments. This research has been supported by the Climate Dynamics Section of the National Science Foundation under Grant ATM-80-24881. We are grateful to Caren Klarman for typing the manuscript, Clare Villanti for preparing the figures, and Hyo Duck Chang for his help in plotting the results on the computer.

REFERENCES

Ashe, S., 1979: A nonlinear model of the time-average axially asymmetric flow induced by topography and diabatic heating. *J. Atmos. Sci.*, **36,** 109–126.

Charney, J. G., and A. Eliassen, 1949: A numerical method for predicting the perturbations of the middle latitude westerlies. *Tellus*, **1,** 38–55.

Crutcher, H. L., and J. M. Meserve, 1970: Selected level heights, temperature and dew points for the Northern Hemisphere. NAVAIR-50-1C-52. [Available from Naval Weather Service Command, Washington Navy Yard.]

Derome, J., and A. Wiin-Nielsen, 1971: Response of a middle latitude model atmosphere to forcing by topography and stationary heat sources. *Mon. Wea. Rev.*, **99,** 564–576.

Döös, B. R., 1962: The influence of exchange of sensible heat with the earth's surface on the planetary flow. *Tellus*, **14,** 133–147.

Egger, J., 1976a: The linear response of a hemispheric two-level primitive equation model to forcing by topography. *Mon. Wea. Rev.*, **104,** 351–363.

——, 1976b: On the theory of steady perturbations in the troposphere. *Tellus*, **28,** 381–389.

Holopainen, E. O., 1973: An attempt to determine the effects of turbulent friction in the upper troposphere from the balance requirements of the large scale flow: A frustrating experiment. *Geophysika*, **12,** 151–176.

Hoskins, B. J., and D. Karoly, 1981: The steady linear response of a spherical atmosphere to thermal and orographic forcing. *J. Atmos. Sci.*, **38,** 1179–1196.

Lau, N. C. L., 1979: The observed structure of tropospheric stationary waves and the local balances of vorticity and heat. *J. Atmos. Sci.*, **36,** 996–1016.

——, and J. M. Wallace, 1979: On the distribution of horizontal transports by transient eddies in the Northern Hemisphere wintertime circulation. *J. Atmos. Sci.*, **36,** 1844–1861.

Manabe, S., and T. B. Terpstra, 1974: The effects of mountains on the general circulation of the atmosphere as identified by numerical experiments. *J. Atmos. Sci.*, **31,** 3–42.

Opsteegh, J. D., and H. M. van den Dool, 1979: A diagnostic study of the time-mean atmosphere over Northwestern Europe during winter. *J. Atmos. Sci.*, **36,** 1862–1879.

——, and ——, 1980: Seasonal differences in the stationary response of a linearized primitive equation model: prospects for long-range forecasting? *J. Atmos. Sci.*, **37,** 2169–2185.

Saltzman, B., 1962: Empirical forcing functions for the large-scale mean disturbances in the atmosphere. *Geophys. Pura Appl.*, **59,** 173–183.

——, 1965: On the theory of the winter average perturbations in the troposphere and stratosphere. *Mon. Wea. Rev.*, **93,** 195–211.

——, 1967: On the theory of the mean temperature of the earth's surface. *Tellus*, **19,** 219–259.

——, 1968: Surface boundary effects on the general circulation and macroclimate: A review of the theory of the quasi-stationary perturbations in the atmosphere. *The Causes of Climate Change, Meteor. Monogr.*, No. 30, Amer. Meteor. Soc., pp. 4–19.

——, and F. E. Irsch, 1972: Note on the theory of topographically forced planetary waves in the atmosphere. *Mon. Wea. Rev.*, **100,** 441–444.

Sankar Rao, M., and B. Saltzman, 1969: On a steady-state theory of global monsoons. *Tellus*, **21,** 308–330.

Smagorinsky, J., 1953: The dynamical influence of large-scale heat sources and sinks on the quasi-stationary mean motions in the atmosphere. *Quart. J. Roy. Meteor. Soc.*, **100,** 342–366.

——, 1963: General circulation experiments with the primitive equations: I, The basic experiment. *Mon. Wea. Rev.*, **91,** 99–164.

Vernekar, A. D., 1975: A calculation of normal temperature at the earth's surface. *J. Atmos. Sci.*, **32,** 2067–2081.

——, and H. D. Chang, 1978: A statistical-dynamical model for stationary perturbations in the atmosphere. *J. Atmos. Sci.*, **35,** 433–444.

Youngblut, C., and T. Sasamori, 1980: The nonlinear effects of transient and stationary eddies on the winter mean circulation. Part 1: Diagnostic analysis. *J. Atmos. Sci.*, **37,** 1944–1957.